JOURNAL OF SPACECRAFT AND ROCKETS
Vol. 35, No. 1, January–February 1998

High-Altitude Capsule Aerodynamics with Real Gas Effects

M. S. Ivanov,* G. N. Markelov,† and S. F. Gimelshein†
Institute of Theoretical and Applied Mechanics, Novosibirsk 630090, Russia
and
L. V. Mishina,‡ A. N. Krylov,‡ and N. V. Grechko‡
RSC ENERGIA, Korolev 141070, Moscow Region, Russia

Re-entry capsule aerodynamics within a wide range of angles of attack and flight altitudes are examined by the direct simulation Monte Carlo method. The local bridging method is verified by comparison with results of simulations. Capsule stability is analyzed for flight altitudes from 130 km down to 85 km. Comparison between computed and free flight data shows a good agreement. A qualitative change of heat transfer coefficient behavior for different angles of attack during the descent is revealed. The influence of chemical reactions on aerodynamics and flowfields at 85 km is shown to be significant. For a flow simulation in the near-continuum regime, a parallel version of the direct simulation code, with static and dynamic load balancing techniques, is used. An efficiency of about 80% is obtained for 256 processors using dynamic load balancing.

Nomenclature

C_A = axial force normalized by $\rho_\infty U_\infty^2 S/2$
C_H = heat transfer normalized by $\rho_\infty U_\infty^3 S/2$
C_m = pitching moment normalized by $\rho_\infty U_\infty^2 SL/2$
C_N = normal force coefficient normalized by $\rho_\infty U_\infty^2 S/2$
c_k = local coefficient
$c_{k,\text{cont}}$ = continuum coefficient
$c_{k,\text{fm}}$ = free molecular coefficient
F_b = bridging function
H = altitude, km
Kn = Knudsen number
$Kn_{0,\infty}$ = Knudsen number based on μ_0, T_0, and ρ_∞
L = characteristic length, m
N_l = number of molecules in cell l
N_m = average number of simulated molecules in the computational domain
N_{proc} = number of processors
S = characteristic size, m^2
T_0 = stagnation temperature, K
t_{calc} = calculation time
t_{com} = communication time
t_{idle} = synchronization time
t_{tot} = total operation time
U_∞ = freestream velocity, m/s
α = angle of attack, deg
ε_l = volume of interaction region in cell l, m^3
μ_0 = stagnation viscosity, kg/m·s
ν_l^m = majorant frequency, s^{-1}
ρ_∞ = freestream density, kg/m^3

Introduction

THE emergence of new capsule programs has lately drawn considerable interest in the aerothermodynamics of these vehicles along the entire flight trajectory. Capsules are widely used for the transportation of payloads to orbital space stations. Accurate information on capsule aerodynamics along the descent trajectory, especially momentum characteristics, allows one to understand the capsule performance and, therefore, increase the payload and reduce the heat-shield thickness on the aeroshell capsule.

Presented as Paper 97-0476 at the AIAA 35th Aerospace Sciences Meeting, Reno, NV, Jan. 6–9, 1997; received Jan. 21, 1997; revision received Aug. 1, 1997; accepted for publication Oct. 9, 1997.

*Head, Computational Aerodynamics Laboratory. E-mail: ivanov@itam.nsc.ru. Senior Member AIAA.
†Research Scientist, Computational Aerodynamics Laboratory.
‡Research Scientist, Aerodynamics Department.

One of the main problems is the capsule static stability. Normally, the capsule instability arises at high altitudes. The stabilization of the capsule attitude usually occurs in the near-continuum regime ($H \sim 90$ km), as the capsule approaches the peak heating. An accurate prediction of aerodynamic characteristics and heat fluxes during the possible tumbling of the capsule on the first stage of re-entry trajectory is therefore of great importance.

The principal goal of the present work is to study the aerothermodynamics of a re-entry capsule from the free-molecular to the near-continuum regimes, in the range of altitudes from 130 km down to 85 km. In this range of altitudes, a considerable redistribution of pressure and friction forces takes place. To obtain realistic data on the capsule aerodynamics in high-temperature flows, the real gas effects have to be taken into account. These effects, which become particularly important for $H = 85$ km, are also discussed in the paper.

Computational Approaches

A combination of engineering tools, experimental means, and numerical methods is used in the design of high-altitude re-entry capsule aerodynamics.

Though commonly used, the low-density, high-enthalpy wind tunnels often suffer from a lack of accuracy due to the small size of models, insufficient accuracy of measurement techniques, and flow nonuniformities. Rarefied gas effects are also difficult to assess by flight experiments due to inaccurate measurements related to weak forces and moments.

Engineering tools usually utilize bridging functions that serve as interpolation between free-molecular models and continuum models. This approach often fails when predicting the center of pressure. It also does not permit one to estimate heat fluxes with a high accuracy.

On the numerical side, the continuum flow theory is no longer valid, and the simulation of low-density flows is based on a kinetic description connected with the Boltzmann equation. The most promising of the kinetic approaches is the direct simulation Monte Carlo (DSMC) method, which is widely used for numerical modeling of low-density flows.

Both DSMC and engineering tools are utilized here to examine capsule aerodynamics for different flow regimes. A combined usage of the two different approaches—the exact but time-consuming DSMC method and the fast but approximate engineering approach—has an evident benefit when studying typically complex three-dimensional capsule flows.

Engineering Approach

For calculating the capsule aerodynamics by the engineering method, the aerodynamic modeling system RAMSES[1] is used, where the local bridging approximation is implemented. Generally,

bridging methods allow one to construct fast engineering codes for aerodynamic calculations in the flow regime between free-molecular and hypersonic continuum conditions. The local bridging methods take advantage of the fact that both limits, namely the free-molecular and the Newtonian continuum, can be described by a local aerodynamic analysis. The aerodynamic coefficients of a local surface element depend only on freestream and local properties, such as the local angle of attack, and local surface interaction.

The same local aerodynamic behavior is also assumed to be applicable in the transitional flow regime. The gap between local continuum and local free-molecular coefficients is bridged by semiempirical functions that in principle are a weighted mix of the known limit values. The weighting function depends on independent correlations or similarity parameters, such as Knudsen number, and is usually determined by analysis of experimental results. One thus assumes for individual local coefficients c_k

$$c_k = c_{k,\mathrm{fm}} F_b(Kn, \alpha, \ldots) + c_{k,\mathrm{cont}}[1 - F_b(Kn, \alpha, \ldots)]$$

For the transitional flow regime, the local bridging provides a dependence of pressure and shear stress coefficients on independent parameters.

In this paper, the generalized, asymmetric $erf - \log Kn$ bridging[2] is used, which allows an asymmetric transition of variable span between continuum and free-molecular flow. For this method,

$$F_b = 0.5\left(1 + erf\left\{\frac{\sqrt{\pi}}{\Delta Kn}\log\left[\frac{Kn_{0,\infty}}{Kn_m(\alpha)}\right]\right\}\right)$$

Two important constants have been introduced here. The first one, Kn_m, determines the Knudsen number at the center of the transitional regime. The center of transition is defined by $F_b = 0.5$ and is obtained for $erf = 0$. The error function has this value for $\log[Kn_{0,\infty}/Kn_m(\alpha)]$, which is the case for $Kn_{0,\infty} = Kn_m$. With the constant Kn_m we, therefore, fix the value of $Kn_{0,\infty}$ at the transition center. The second constant, ΔKn, gives the logarithmic width of the transitional regime.

Kinetic Approach

The DSMC method is conventionally regarded as a phenomenological method of physical simulation of rarefied flows.[3] Conversely, the statistical simulation method is constructed directly from the spatially nonuniform master Leontovich kinetic equation for the N-particle distribution function.[4] Because the Boltzmann equation can be derived from the master kinetic equation for an N-particle system under the conditions of molecular chaos, the DSMC method is regarded as a numerical method for solving the Boltzmann equation.

The majorant cell and free cell frequency schemes[4] of the DSMC method were used in the computations. In the present paper, the following combined method is applied.[5] The computational domain is divided into uniform Cartesian background cells. The time between consecutive collisions τ is simulated for each background cell from the probability density $\nu_m \exp\{-\nu_m \tau\}$. Here, the majorant frequency of collisions is

$$\nu_l^m = \frac{N_l(N_l - 1)}{2}[\sigma(g)g]_{\max}\frac{1}{\varepsilon_l}$$

The exponential form for τ allows one to accurately model the collision process for a small number of particles in a cell. The linear size of the background cells is specified to be approximately equal to the freestream mean free path. An interaction region, defined by ε_l, governs the local collision resolution. In an undisturbed flow, an interaction region coincides with a background cell. In other flow regions, the linear size of an interaction region is adapted to the local mean free path during the modeling process. In fact, the interaction region is a virtual cell and similar to a cell in the cell scheme. Thus, there are two kinds of fictitious collisions. The first kind is connected with a distance between particles to be collided and is defined by the interaction region, and the second one is due to the relative collision velocity g.

The inclusion of the density gradient enables us to decrease the linear size of a virtual cell along the direction of flow gradient to enhance the grid resolution. The combined use of cell (background cells) and free cell (virtual cells that are smaller than background cells) makes it possible to achieve adequate spatial resolution in the entire flowfield. In conjunction with the correct collision number for even small number of particles in a cell, this allows one to simulate the flow at very small Knudsen numbers.

The use of the DSMC method for solving complicated practical problems at flight altitudes of 120–300 km is relatively straightforward from the computational viewpoint. However, the simulation of flows at altitudes of 80–120 km faces extra difficulties due to the following factors: physical and chemical processes and high gas density leading to a high number of molecular collisions.

To simulate the physical peculiarities of high-temperature airflow about a capsule, the following models were used: a variable soft sphere[6] (VSS) model for intermolecular potential, the Larsen–Borgnakke model[7] with discrete rotational[8] and vibrational[9] energies for energy exchange between translational and internal modes of molecules, and a chemical reaction model[10] that takes into account vibration-dissociation coupling.

Air is considered as a five-species gas mixture (N_2, O_2, NO, N, and O) with 15 dissociation and 4 exchange reactions. The parameters for VSS intermolecular interactions are taken from Ref. 3. The diffuse law is taken for gas–surface interaction with complete accommodation of translational and internal energies.

To overcome computational difficulties related to the reduction of the Knudsen number, the parallel version of the DSMC code with the domain decomposition for load balancing (LB)[11] was used to simulate three-dimensional rarefied flows around the capsule at the altitudes of 90 and 85 km. Parallel computers are currently the only means for obtaining accurate data in the near-continuum flow regime with the DSMC method.

Parallel DSMC Strategies

The DSMC parallelization is traditionally based on domain decomposition. Its essence is the partitioning of the computational domain into subdomains and the allocation of each subdomain to a particular processor. The processes of particle collision and transport are simulated independently in every subdomain, and the exchange of information between the subdomains is carried out by transferring the particles that leave the subdomain to another processor.

The total time of the processor operation is $t_{\mathrm{tot}} = t_{\mathrm{calc}} + t_{\mathrm{com}} + t_{\mathrm{idle}}$. The principal goal of parallelization is to minimize t_{com} and t_{idle}. The time of calculation t_{calc} depends on the number of particles in each subdomain, the number of collisions, and the presence of a body. This significantly complicates the procedure of subdividing into subdomains because a large difference in t_{calc} for various processors causes a strong increase in t_{idle}. The main method of decreasing the difference in t_{calc} is the use of a load balancing.

The main LB types are 1) static, where the domain is partitioned before the computation, and 2) dynamic, where the balancing of processors is performed during the computation. Both the static and dynamic LB techniques are used in this paper. The neighboring background cells are united into groups, so-called clusters, that are the minimum spatial unit; these are distributed and transferred between the processors. The algorithms used in the present work are scalable and require only local, not global, knowledge of the load distribution in a system.

1) Static LB: The probabilistic approach of cluster allocation is used here. The main advantages of this approach are its low cost and fairly good balancing for a small number of processors ($N_{\mathrm{proc}} \leq 64$). The basic drawback is the violation of data locality: Each processor has clusters located in different places of the computational domain, and in the general case its neighbors are all other processors; the large number and size of communications between the processors result in a sudden drop of efficiency when increasing the number of processors.

2) Dynamic LB: A uniform distribution of clusters between the processors is initially assumed. As the flow structure changes, the clusters are redistributed between neighboring processors in the physical network. The data locality is conserved, and the amount of work and direction of its transfer are determined by the heat diffusion procedure.[12]

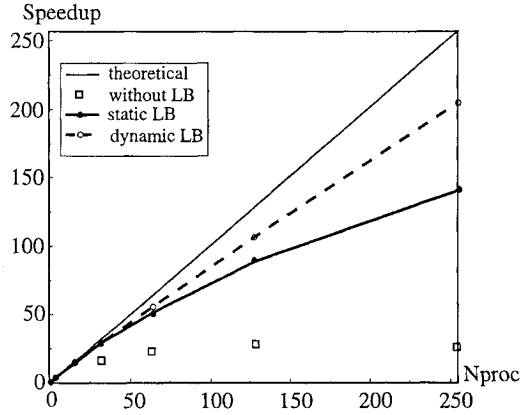

Fig. 1 Speedup for different LB techniques.

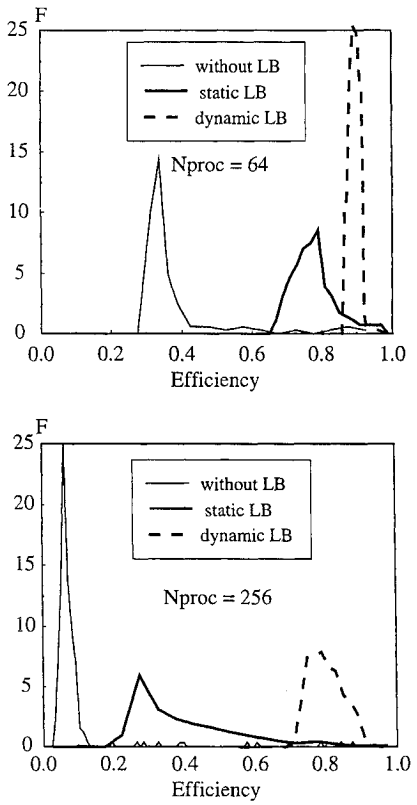

Fig. 2 Distribution function of the number of processors vs efficiency.

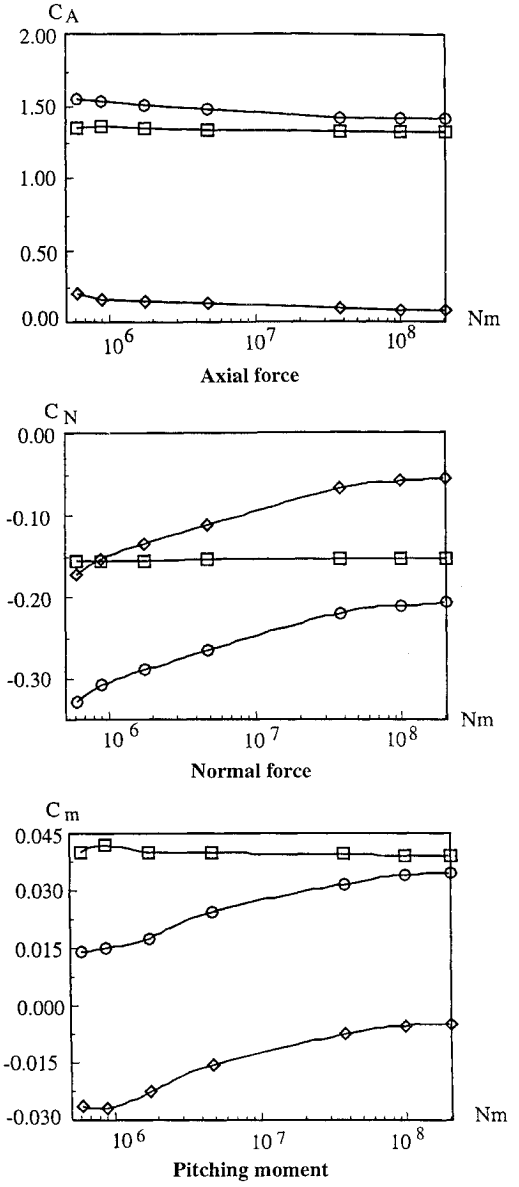

Fig. 3 Influence of the number of particles: ○, total; □, pressure contribution; and ◊, friction contribution.

The main results on the DSMC parallelization of computations of the flow about a capsule at the altitude of 85 km are summarized next.

As a result of the large difference in workload for each cluster, the overall speedup of the computation is quite low for standard spatial decomposition without LB (about a factor of 25 for 256 processors). The speedup increases dramatically when the LB techniques are used. Figure 1 shows the speedup as a function of the number of processors for static and dynamic LB. The difference between the two approaches is negligible if a small number of processors ($N_{\text{proc}} \leq 64$) is used. If the number of processors is increased up to 256, the difference accounts for 30%.

Figure 2 presents the distribution of the number of processors vs $t_{\text{calc}}/t_{\text{tot}}$ for various types of LB. In all cases the reduction of efficiency is related to the presence of a few processors whose calculation time is much larger than the calculation time of other processors. This is especially noticeable for computations without LB and also for static LB at $N_{\text{proc}} = 256$.

The main reason for the imbalance and the difference of computed and theoretical speedup is the difference in t_{calc} rather than in t_{com}. The communication time is small because of both a high speed of data transfer and a small volume of transferred data. For 256 processors and dynamic LB the maximum number of transferred molecules was less than 1% of the total number of molecules. Further speedup improvement can be achieved by balancing t_{calc} through the cluster exchange aimed at exact correspondence to the amount of work to be transferred.

An important argument for using parallel computers in the DSMC computations of three-dimensional flows in the near-continuum regime ($Kn < 0.01$) is a strong dependence of distributed and total aerodynamic characteristics on the number of simulated particles. Figure 3 shows the aerodynamic characteristics C_A, C_N, and C_m for different N_m ($H = 85$ km and $\alpha = -20$ deg). The analysis of the contribution of pressure and friction forces to the aerodynamic characteristics shows that the friction forces are very sensitive to N_m. If the number of particles is not large enough, this causes a significant increase in the number of repeated collisions, i.e., collisions of the same pairs of particles repeated many times during their lifetime. Such an increase amplifies the statistical dependence between model particles. In fact, this reduces the number of effective collisions and, therefore, increases an effective Knudsen number.

The number of collision cells may also affect simulation results, and particular attention has therefore been paid to provide for adequate grid resolution. For computations of flows at altitudes higher than 90 km, virtual cells whose linear size is smaller than the local mean free path were used. When computing flows at 90 km, and especially 85 km, though, the number of collision cells is enormous even for modern parallel computers. The use of the free cell

scheme allows one to weaken the requirements for computer memory. However, the utilization of a huge amount of virtual cells results in a significant increase in the computational time. An analysis of the effect of grid resolution on simulation results has therefore been performed. The study is conducted for $H = 85$ km, $\alpha = -20$ deg, and $N_m = 38 \times 10^6$. When decreasing the number of virtual cells from 40×10^6 to 20×10^6, the results did not change, but further decreasing down to 5×10^6 gives a change of 1% in total aerodynamic characteristics. To avoid any influence of the grid, the other computations are conducted with 20×10^6 virtual cells.

Results and Discussion

Aerodynamic Coefficients

Both the kinetic and engineering methods were applied here. The comparison of aerodynamic coefficients C_A and C_N (Figs. 4 and 5) obtained by two different methods shows that the accuracy of the local bridging predictions lies within 5%, which is quite suitable for practical applications. The contribution of pressure forces to these characteristics is weakly dependent on the flight altitude, and the contribution of friction forces decreases during the descent (Fig. 6).

Both numerical approaches yield a similar behavior of the pitching moment coefficient C_m as a function of the flight altitude (Fig. 7). At high flight altitudes the capsule is statically unstable at the zero

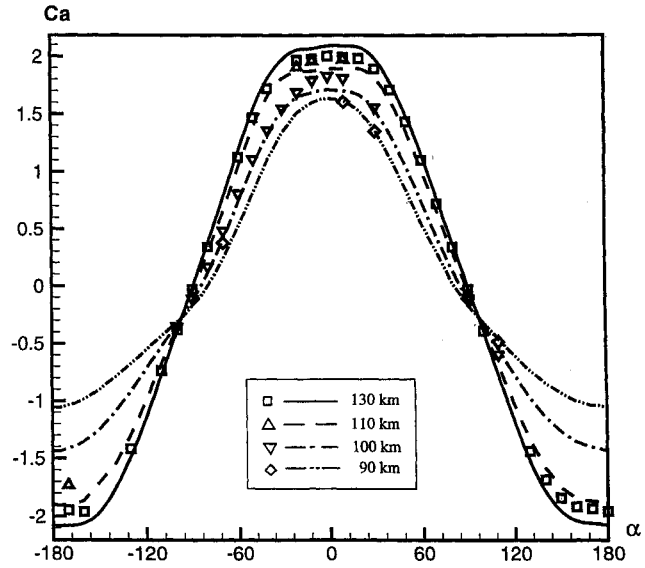

Fig. 4 Axial force coefficient for different flight altitudes: symbols, DSMC and curves, bridging.

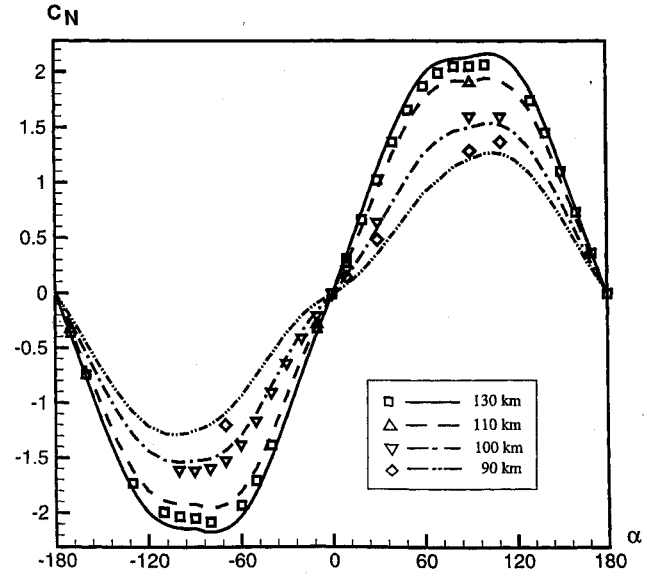

Fig. 5 Normal force coefficient for different flight altitudes: symbols, DSMC and curves, bridging.

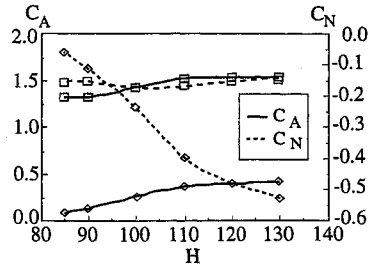

Fig. 6 Pressure and skin-friction contributions to axial and normal forces for $\alpha = -20$ deg: □, pressure contribution and ◇, friction contribution.

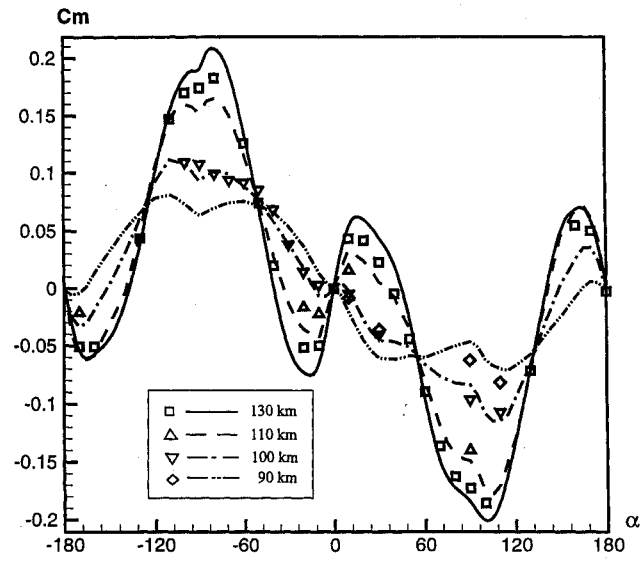

Fig. 7 Pitching moment coefficient for different flight altitudes: symbols, DSMC and curves, bridging.

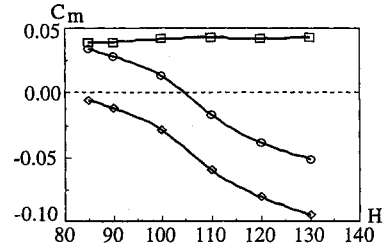

Fig. 8 Pressure and skin-friction contributions to pitching moment for $\alpha = -20$ deg: ○, total; □, pressure contribution; and ◇, friction contribution.

angle of attack, and its stabilization takes place at an altitude of ~90 km. This is explained by the redistribution of pressure and friction forces as altitude is decreased (Fig. 8). The pressure gives a positive contribution to C_m, whereas the friction forces give a negative one, which is substantially reduced along the descent trajectory.

The difference in the pitching moment coefficient C_m predicted by the local bridging method from the DSMC results is rather considerable (~20%) around the angles of attack where the static stability parameter $\partial C_m/\partial\alpha$ is close to zero. Near the trim angle, the absolute values of C_m are very small, and the local bridging method does not permit a credible estimate of qualitative behavior of C_m. For instance, at $\alpha = -10$ deg and $H = 100$ km the local bridging method yields $C_m < 0$, whereas the DSMC value is $C_m > 0$. Therefore, for a detailed analysis of capsule aerodynamics, the DSMC method should be used to correct the local bridging predictions.

Comparison with Experiment

The comparison of both DSMC and engineering data with free-flight results[13] was made for the altitude of $H = 85$ km. The force and torque coefficients predicted with the DSMC method are in excellent agreement with free-flight ones for the whole range of variation of the angle of attack (Fig. 9). The local bridging gives C_A and C_N coefficients that are rather close to the DSMC values. Meanwhile, the difference in C_m is significantly larger, and the minimum in C_m observed at ≈ -80 deg is shifted for local bridging to ≈ -90 deg. This again shows an evident need for the DSMC method instead of

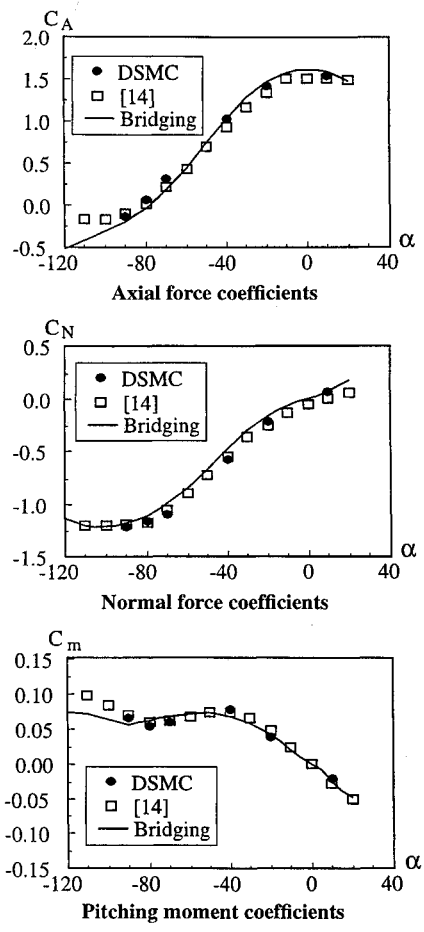

Fig. 9 Comparison of computed and experimental data.

the local bridging to accurately predict aerodynamic characteristics, even for a relatively simple convex configuration.

Heat Fluxes

One of the important characteristics for re-entry capsules is the heat flux on the body. An accurate prediction of the flow is necessary for the determination of heat fluxes because these fluxes have a direct impact on selection of the material for the thermal protection system. To obtain credible information on the heat transfer coefficient of a capsule in the transitional regime, the DSMC method has to be used.

The results of computation of the heat transfer coefficient are presented in Fig. 10 for different altitudes. For $H = 130$ km, where the flow regime is close to free molecular ($Kn \approx 4.5$), the dependence of C_H on α is influenced only by the area of the windward side of the body. The smallest area of the windward side corresponds to $\alpha = 0$, and the local minimum is observed for $\alpha = -90$ deg.

The behavior of C_H alters qualitatively near $\alpha = 0$ for the altitude $H = 100$ km ($Kn \approx 0.04$). In this case, the minima occur at $\alpha = \pm 20$ deg and the local maximum exists for $\alpha = 0$. Unlike $H = 130$ km, a shock wave is formed, and the distance from the shock to the body plays an important role for C_H distribution. When the angle of attack is changed from 0 to -20 deg (Figs. 11a and 11b), the maximum of heat flux is observed near the top edge of the forebody. The heat flux is lower on the other portion of the forebody as compared with that for $\alpha = 0$ because of the larger shock standoff distance. All of this causes the reduction of the total C_H.

The further change of the angle from -20 to -40 deg (Figs. 11b and 11c) results in the decrease of C_H on the forebody. Nevertheless, the total C_H grows due to the increase of heat flux on the upper side of the body.

Real Gas Effects

In high-velocity flows about a capsule, as the fluid is heated and compressed through the shock, conditions are reached whereby

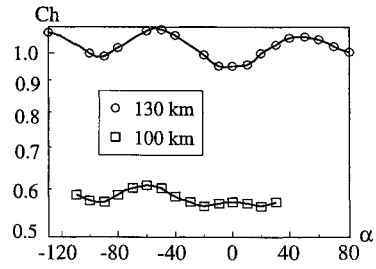

Fig. 10 Total heat transfer coefficient.

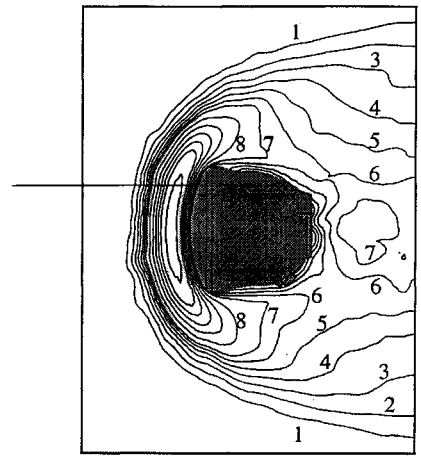

a) 0 deg

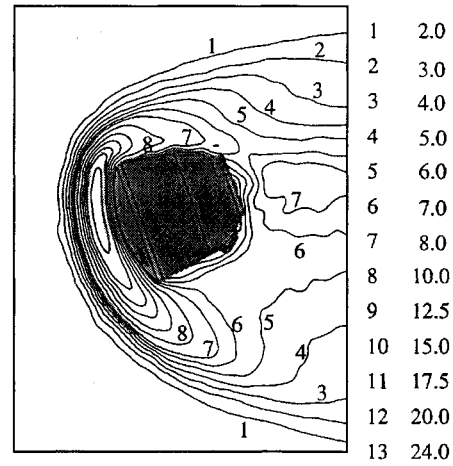

b) −20 deg

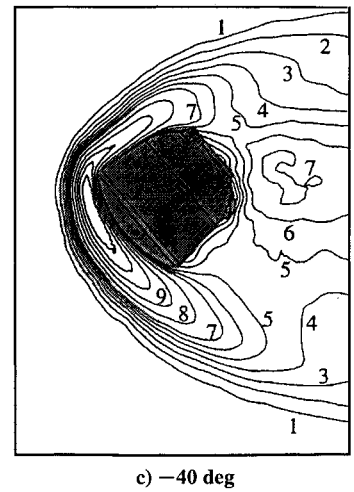

c) −40 deg

Fig. 11 Temperature flowfields; H = 100 km.

Table 1 Aerodynamic characteristics for $H = 85$ km and $\alpha = -20$ deg

Case	C_A	C_N	C_m	C_h
Nonreactive air	1.42	−0.22	0.032	0.19
Reactive air	1.45	−0.22	0.033	0.10

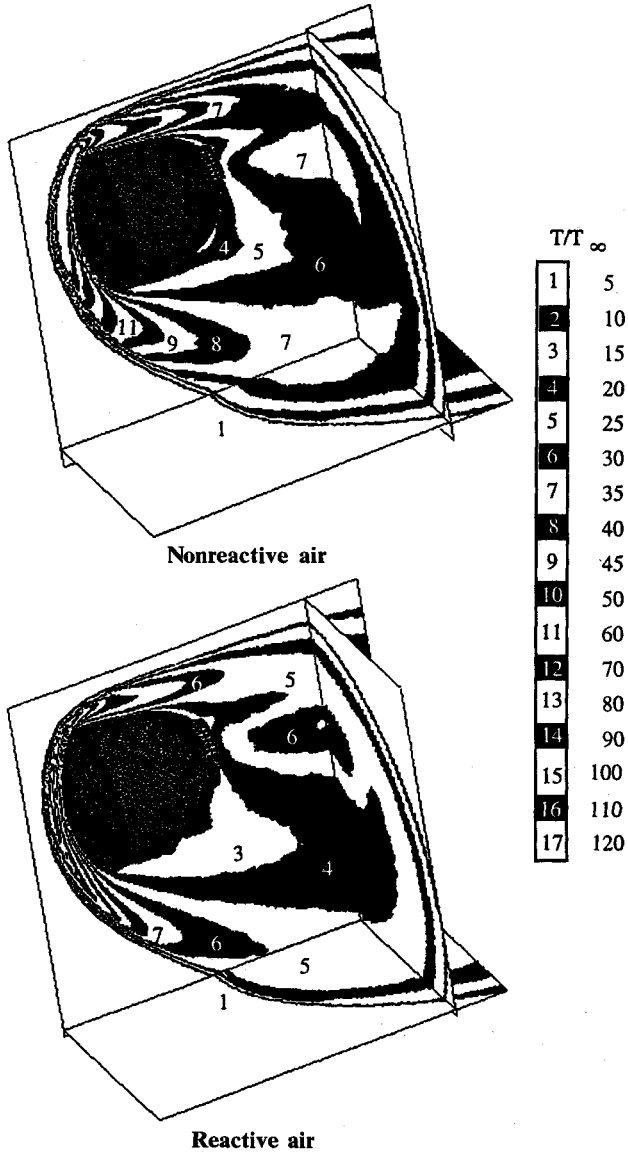

Fig. 12 Temperature flowfields; $H = 85$ km.

chemical reactions take place. These reactions are of great importance for altitudes lower than 90–100 km because they can alter the flowfield locally through the production of energy, chemical species, etc.

The impact of chemical reactions on aerothermodynamic coefficients of a capsule at the altitude of $H = 85$ km is shown in Table 1. For this altitude, the coefficients C_A and C_N are nearly the same for reactive and nonreactive air. The pitching moment coefficient decreases by ~4%. The coefficient C_H is most sensitive to chemical reactions, and its decrease amounts to 90%.

An example of the influence of chemical reactions on the flowfield structure is given in Fig. 12. A considerable difference is observed both in the bow shock standoff distance and in the wake flow structure. Obviously, the temperature reduction behind the shock wave for chemically reactive gas is rather large. The mole fractions of air atomic species, nitrogen and oxygen, are presented in Fig. 13. Oxygen is fully dissociated near the forebody, and the degree of dissociation of molecular nitrogen approaches 30%.

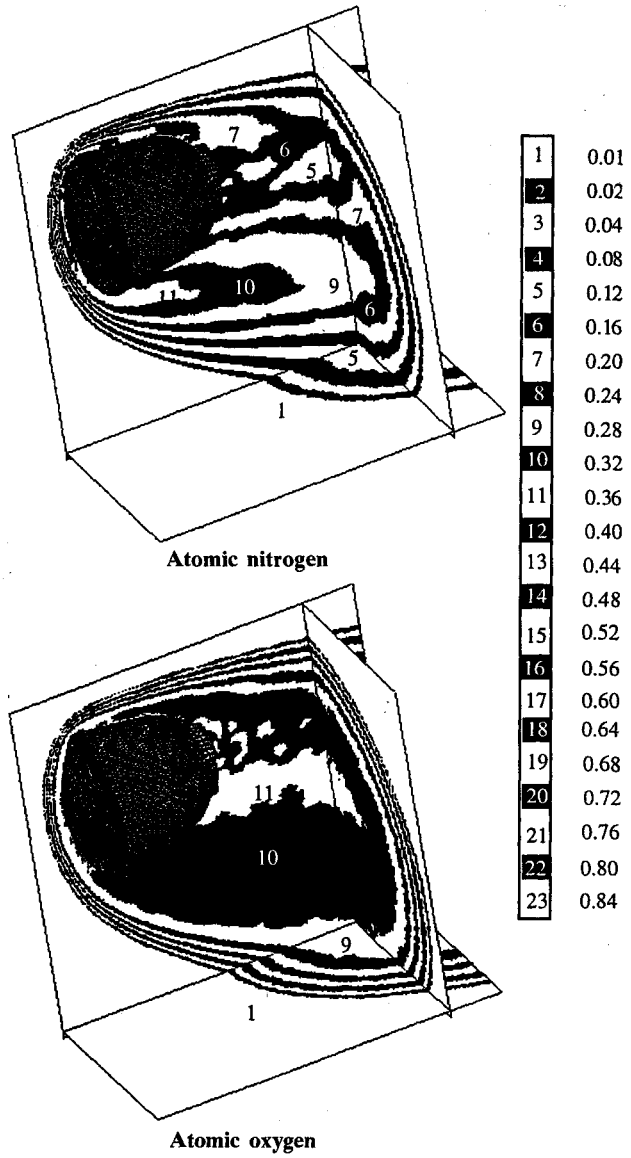

Fig. 13 Mole fraction flowfields for reactive air; $H = 85$ km.

Conclusions

Capsule aerodynamics have been examined numerically for various angles of attack ($0 < \alpha < 360$ deg) from free-molecular to near-continuum flow regimes. The main computations were conducted with the DSMC method. Parallel DSMC code with static and dynamic load balancing techniques was used to compute the flows at altitudes of 85 and 90 km. A high efficiency of dynamic load balancing for a large number of processors was proven. The actual number of simulated particles on capsule aerodynamics was shown to be critical. To obtain accurate data for the altitude of 85 km, about 100×10^6 particles have to be taken.

The calculations were also carried out by the local bridging method. The engineering approach allows one to quickly estimate the overall behavior of aerodynamic characteristics, whereas the DSMC method can be used to generate detailed data, especially in the range of angles of attack where the engineering method loses accuracy.

Capsule stability was examined at various flight altitudes. It is shown that, when decreasing the altitude, the capsule instability, caused mainly by friction forces, decreases. At altitudes below $H = 90$ km the capsule becomes stable.

The aerodynamic characteristics obtained by the DSMC method are in very good agreement with the free-flight data for the altitude $H = 85$ km. The local bridging gives axial and normal force coefficients that are in reasonable agreement with both experimental and DSMC results, but the pitching moment significantly differs.

Dependence of the heat transfer coefficient on the angle of attack for different altitudes was studied. During descent, the minimum of heat transfer shifts from $\alpha = 0$ ($H = 130$ km) to $\alpha = -20$ deg ($H = 100$ km).

Computations of chemically reactive flows about a capsule were performed. The influence of chemical reactions becomes stronger when the altitude decreases from 130 to 85 km. The most pronounced changes, due to the chemical reactions in air, are observed for the heat transfer coefficient, which drops considerably (by a factor of almost 2). Aerodynamic coefficients of normal force, axial force, and pitching moment change by a few percent.

References

[1]Koppenwallner, G., Johannsmeier, D., Klinkard, H., Ivanov, M., and Kashkovsky, A., "A Rarefied Aerodynamics Modelling System for Earth Satellites (RAMSES)," *Proceedings of the XIX International Symposium on Rarefied Gas Dynamics*, edited by J. Harvey and G. Lord, Oxford Univ. Press, Oxford, England, UK, 1995, pp. 1366–1372.

[2]Shelkonogov, A., and Koppenwallner, G., "Free Molecular and Transitional Aerodynamics of Spacecraft. Local Bridging Methods," ESOC Contract 10032/92/D/IM, Hypersonic Technology Goettingen, Lindau/Harz, Germany, March 1994.

[3]Bird, G. A., *Molecular Gas Dynamics and Direct Simulation of Gas Flows*, Oxford Univ. Press, New York, 1994, pp. 208–217.

[4]Ivanov, M. S., and Rogasinsky, S. V., "Theoretical Analysis of Traditional and Modern Schemes of the DSMC Method," *Proceedings of the XVII International Symposium on Rarefied Gas Dynamics*, edited by A. E. Beylich, VCH Veinheim, 1991, pp. 629–642.

[5]Ivanov, M. S., Antonov, S. G., Gimelshein, S. F., and Kashkovsky, A. V., "Computational Tools for Rarefied Aerodynamics," *Proceedings of the XVIII International Symposium on Rarefied Gas Dynamics*, edited by B. D. Shizgal and D. P. Weaver, Vol. 160, Progress in Astronautics and Aeronautics, AIAA, Washington, DC, 1994, pp. 115–126.

[6]Koura, K., and Matsumoto, H., "Variable Soft Sphere Molecular Model for Inverse-Power-Law of Lennard-Jones Potential," *Physics of Fluids A*, Vol. 3, No. 10, 1991, pp. 2459–2465.

[7]Borgnakke, C., and Larsen, P. S., "Statistical Collision Model for Monte Carlo Simulation of Polyatomic Gas Mixture," *Journal of Computational Physics*, Vol. 18, No. 4, 1975, pp. 405–420.

[8]Boyd, I. D., "Relaxation of Discrete Rotational Energy Distributions Using a Monte Carlo Method," *Physics of Fluids A*, Vol. 5, No. 9, 1993, pp. 2278–2286.

[9]Bergemann, F., and Boyd, I. D., "DSMC Simulation of Inelastic Collisions Using the Borgnakke-Larsen Method Extended to Discrete Distributions of Vibrational Energy," *Proceedings of the XVIII International Symposium on Rarefied Gas Dynamics*, edited by B. D. Shizgal and D. P. Weaver, Vol. 158, Progress in Astronautics and Aeronautics, AIAA, Washington, DC, 1994, pp. 174–183.

[10]Gimelshein, S. F., Gorbachev, Yu. E., Ivanov, M. S., and Kashkovsky, A. V., "Real Gas Effects on the Aerodynamics of 2D Concave Bodies in the Transitional Regime," *Proceedings of the XIX International Conference on Rarefied Gas Dynamics*, edited by J. Harvey and G. Lord, Oxford Univ. Press, Oxford, England, UK, 1995, pp. 556–563.

[11]Ivanov, M., Markelov, G., Taylor, S., and Watts, J., "Parallel DSMC Strategies for 3D Computations," *Proceedings of the Parallel CFD'96 Conference*, edited by P. Schiano, A. Ecer, J. Periaux, and N. Satofuka, North-Holland, Amsterdam, 1997, pp. 485–492.

[12]Taylor, S., Watts, J., Rieffel, M., and Palmer, M., "The Concurrent Graph: Basic Technology for Irregular Programs," *IEEE Parallel and Distributed Technology*, Vol. 4, No. 2, 1996, pp. 15–25.

[13]Reshetin, A. G., and Semenov, Yu. P., "Investigation Aerodynamic Characteristics of Space Vehicle," *Proceedings of the III All-Union School on Methods of Aerophysical Research*, edited by A. M. Kharitonov, Inst. of Theoretical and Applied Mechanics, Novosibirsk, Russia, 1982, pp. 10–14 (in Russian).

I. D. Boyd
Associate Editor